EFFECT OF ENVIRONMENTAL FACTORS ON MECHANICAL PROPERTIES OF RESIN, INTERFACE AND COMPOSITES

Sagar M. Doshi, Alex Schneider, Paul D. Samuel,
Joseph M. Deitzel,
Center for Composite Materials, University of Delaware, Newark, DE

John W. Gillespie Jr.
Center for Composite Materials, University of Delaware, Newark, DE
Department of Civil and Environmental Engineering, Department of Mechanical Engineering, Department of Materials Science and Engineering, and Department of Electrical and Computer Engineering, University of Delaware, Newark, DE

Abstract

Composites are used increasingly for automotive applications where they are subjected to various environmental conditions, from different temperatures to varying humidity. The environmental conditions influence the composite's structural and energy absorbing properties. Composites used in automotive applications need to be damage tolerant and may also be designed for energy absorbing parts in crash scenarios where they may be subjected to strain rates of ~100-1000 1/s. In this research, we discuss a framework to study environmental factors' effect on composite materials' performance by characterizing neat epoxy resin, interface, and glass-epoxy composites.

A toughened epoxy resin, SC-15, is used in this study, where the key mechanical properties such as yield stress and Young's modulus are characterized at quasistatic and high strain rates (using Hopkinson bar) at different temperatures and moisture conditions. An Eyring type curve is generated to predict properties at varying strain rates. Interfacial properties between the SC-15 resin and 463-sized glass fiber are characterized using a single fiber pullout test at the ends of the operating temperature range (-55C, 76C) and moisture conditioning. Lastly, composite panels are subjected to low velocity impact tests at operating temperatures. Force displacement, force-time, stiffness before and after impact, and delamination area are analyzed for each specimen. A correlation is shown between key resin properties such as yield strength with the apparent interfacial shear strength calculated through pullout tests and the stiffnesses of the composite panels with the resin Young's modulus. A detailed study of the testing of composites and their constituent materials is conducted under a wide range of environmental conditions to understand the effect on performance and durability.

Introduction

The amount of polymer composites used in automotive applications is increasing to keep up with the demands of making lightweight, crash-worthy automotives. Other advantages such as near net shape manufacturing, corrosion resistance, and decreasing costs of raw materials also lead to an increased usage of composites. Epoxy resins are commonly used in structural composites due to their ease of manufacturing (pressure required due to low viscosities and cure temperatures), thermal stability, and mechanical properties. However, unlike sheet metal used in traditional automotives, the properties of epoxy resins and their composites change significantly due to environmental conditions such as temperature and moisture.

The operating temperature range for automotive applications is vast due to geographical location changes, altitudes, and in some cases, proximity to power units. For example, per AEC-Q100 (Automotive Electronics Council) qualification test standards, there are different grades defining the operating temperature range from -40C to 150C for Grade 0 and -40C to 85C for Grade 3. Per MIL 810 STD, -51C [1] has been reported in cold conditions, and the maximum temperatures could be as high as 71C. However, the temperature that a composite material may be exposed to could be higher due to other factors such as solar radiation and closeness to heat-producing automotive components. In addition to temperatures, high relative humidity could also severely influence the composites' properties and performance. Not only could it lead to hygrothermal stresses, but the presence of moisture in the polymer could suppress the glass transition temperature and therefore deteriorate the performance at elevated temperatures.

In addition to external environmental factors, the key properties of a polymer composite material are also dependent on the rate of loading or strain rates. For example, composites designed for energy-absorbing structures in the event of a crash may be subjected to strain rates as high as 500 s^{-1}. However, the local strain rates could be even higher, and Smerd et. al. [2] conducted their test at strain rates as high as 1500s^{-1}. It is therefore necessary to study and evaluate the fundamental mechanical properties at various strain rates, from quasistatic to high strain rates. The complete set of properties would enable the creation of more accurate finite element models to determine the crashworthiness of critical components.

Not only do the properties of the epoxy resin matter, but also the bonding between the epoxy resin and the reinforcing material such as glass or carbon fiber. The interfacial properties play a significant role in energy dissipation mechanisms and maintaining the composites' structural integrity. The energy absorbed depends on multiple mechanisms ranging from delamination to fiber break and matrix plasticity, and interfacial debonding. Ganesh et. al. [3] showed that the energy absorbed after a dynamic single fiber break depends on matrix properties (yield strength) and interfacial properties. It is therefore essential to characterize the interfacial properties under different environmental conditions and varying strain rates. Tamrakar et. al. characterized the strain rate-dependent interfacial properties for glass-epoxy composites using a microdroplet test [4].

In this study, we characterize the properties of a toughened epoxy resin SC-15 at quasistatic and high strain rates at various temperatures covering the operating range. Specimens are also tested after saturating with moisture. Eyring curves are generated to show the capability to predict yield stresses across a wide range of strain rates, from quasistatic to high strain rates, which cover the critical strain rates of interest from an automotive viewpoint. Single fiber pullout tests are conducted at different temperatures and conditioned with moisture. Apparent interfacial shear strength (IFSS*) is determined as a function of the temperature. Lastly, low velocity impact tests are conducted on 8-ply composites made of S2 glass fabric with SC-15 epoxy resin. These tests are performed at the ends of the operating temperature range, and key results such as the force-displacement, force-time, delamination areas, and stiffness retention are discussed.

Experimental

The key objective of this study is to test composites and their constituent materials – resin and interface under different environmental conditions. Neat resin is tested using uniaxial compression tests at quasistatic and high strain rates (Figure 1a). The interface is characterized using single fiber pullout tests, and the composites are subjected to low velocity impact testing. The operating temperature for this study is considered to be from -55C to 76C based on [1]; however, some resin testing is also conducted at 95C. The table below summarizes the tests conducted in this study and the parameters used. Note that some additional compression tests (not mentioned in

the table) for neat resin at different strain rates were also done to generate the Eyring curve (yield stress-strain rate relationship).

Table 1: Test configurations and testing parameters for the experiments conducted for resin, interface, and composites testing in this study.

Test Type	Specimen Geometry	Test Conditions	Rate/energy	Equipment Used
Compression of neat resin	Right cylinder, 5mm dia, 5mm thick	-55 to 76C, 95C, moisture saturated (2.1% by weight)	0.1 s^{-1}	Instron 4484
Compression of neat resin	Right cylinder, 5mm dia, 1mm thick	-55 to 76C, 95C, moisture saturated (2.1% by weight)	3300 s^{-1}	Split Hopkinson Bar, REL inc.
Single Fiber Pullout Tests	Single glass fiber embedded in resin	RT dry, RT with moisture conditioning (~2.7% by weight when tested)	0.1 mm/min, embedded length ~ 57 µm	Favimat - TexTechno
Single Fiber Pullout Tests	Single glass fiber embedded in resin	-55C, 76C	0.1 mm/min	Instron 5848 with temp. chamber
Low velocity impact testing	100mm x 150mm x 5mm thick (8 plies)	-55C, RT, 76C	40 Joules	Dynatup 9200 drop tower
Composite stiffness testing	100mm x 150mm x 5mm thick (8 plies)	-55C, RT, 76C	1.27 mm/min	Instron 4484

Materials

The resin system used for this study is a two-part epoxy resin, SC-15, which is rubber toughened low viscosity resin suitable for vacuum-assisted resin transfer molding (VARTM). SC-15 has a glass transition temperature of 85~90C as measured by DSC (mid-point). S2 glass fabric, plain weave (style 240, 814 gm/m^2) with 463 silane-based sizing, which is compatible with epoxy resin, is used. Single fibers used for interfacial testing are of the same type. However, they are cut from a roll of fiber tow procured separately and not pulled from the woven fabric.

Specimen Fabrication and Conditioning

SC-15 part A and part B were weighed in the ratio of 100:30 and then mixed using a high-speed mixer at 2000 rpm, followed by degassing. The resin is then poured between parallel glass plates. The cured resin is cut into cylindrical specimens using a core drill. The diameter of all specimens is 5 mm. The thickness used for quasistatic specimens is 5 mm and 1 mm for SPHB.

For preparing specimens for single fiber pullout testing, the resin was mixed using the same process. The resin was then transferred into customized crucibles with a micropipette, dispensing about 10 µL for each specimen. The fiber was embedded in the resin filled crucible using Textechno FIMABOND equipment. A single glass fiber was inserted in a hollow needle and inserted into the resin droplet using a stage driven by a stepper motor (Figure 1b). The samples were partially cured in-situ until the resin gelled and then batch cured in an oven. All specimens – composites, pullout, and resin, were cured for 2 hours at 60C, followed by post-curing for 4 hours at 121C. The composite specimens were prepared using a conventional VARTM procedure using eight plies of the plain weave S2 glass fabric, with a nominal fiber volume fraction around ~54% measured using burnoff tests. Specific details about VARTM processing for these types of panels are discussed in this research [5].

For neat resin specimens, the conditioning was done in an environmental chamber set to 76C and 88% RH. The samples were conditioned till they reached saturation (a mass increase of 2.1%). For pullout tests, the conditioning was done in a hot water bath maintained at 76C because the air convection in the environmental chamber damaged the specimen.

Testing Methodology

A screw-driven testing machine (Instron 4484) was used for quasistatic testing in a displacement-controlled setting. For high strain rate testing, a split Hopkinson pressure bar was used. For additional details about both quasistatic testing and parameters used for Hopkinson bar testing, please refer to our prior work [6].

Room temperature pullout tests were conducted using FAVIMAT, and tests at elevated/low temperatures were conducted using an Instron MicroTester 5848 equipped with a temperature chamber (Figure 1b). After the completed test, the pulled fiber is collected using a sticky tape and analyzed using an SEM microscope to measure the fiber diameter and embedded length. The interfacial shear stress is calculated by dividing the peak force by the embedded surface area, given by the equation below:

$$IFSS = \frac{Peak\ Load}{Embedded\ Surface\ Area} = \frac{P}{\pi * d * L_e} \quad (1)$$

Where P is load, d is the fiber diameter, and L_e is the embedded length of fiber in resin. Please refer to Chen et. al. [7] for additional details about single fiber pullout testing.

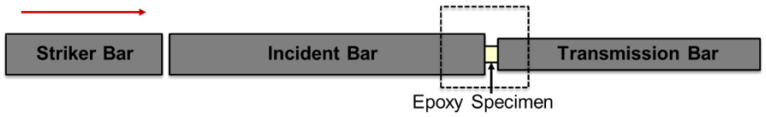

(a)

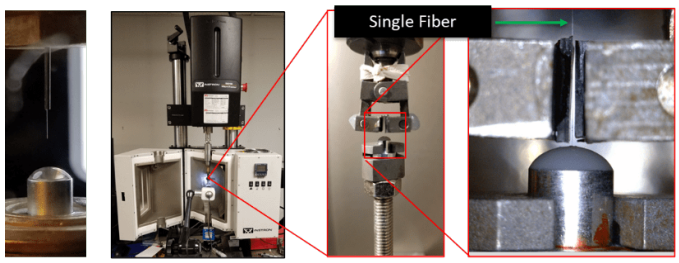

(b)

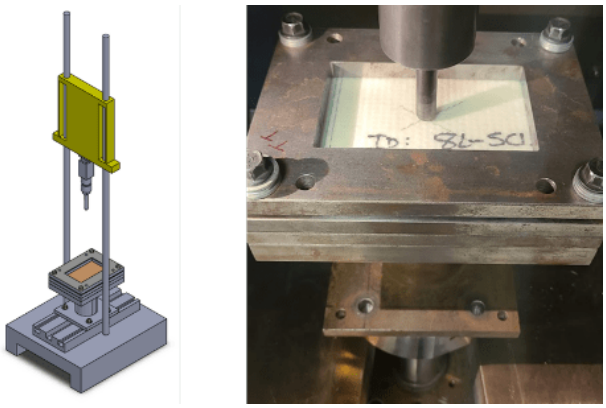

(c)

Figure 1: (a) A schematic of the split Hopkinson pressure bar used for high rate testing, (b) photographs showing the sample preparation and testing for single fiber pullout tests, and (c) a schematic of the drop tower used for LVI testing and photograph of the test setup used for measuring the stiffness of composites.

For LVI testing, a Dynatup 9200 drop tower with a 20,000 lb load cell is used. A variable mass slider (set to 13.37 kg) and a hemispherical tup, 12.7 mm in diameter, is released from a height of ~0.3 m to create an impact with the energy of 40J. The specimen is clamped in the fixture using four bolts at the corners tightened to a torque of 75 lb-in. The impact velocity was measured using an external sensor and was 2.4 m/s. The dropped weight is manually caught after the first impact to prevent additional impacts/damage. For more details about the experimental procedure, stiffness testing, and data reduction procedure, please refer to our prior work [8].

Results and Discussion

Quasistatic and High Strain Rate Testing of Neat Resin

Figures 2(a) and 2(b) shows the true stress-true strain relationship for the quasistatic compressive tests for baseline and conditioned specimens. The machine compliance was measured for the specific test setup and subtracted from the stress-strain response. The slope of the linear part in the initial section of the true stress-true strain curve is used to calculate the modulus. Yield stress is calculated when the stress-strain curve's derivative first goes to zero. The shape of the curves and the general trend is similar for both sets of graphs. After the initial linear increase, the curve is non-linear till it reaches a peak, which is the yield stress. This is followed by strain softening, followed by plastic flow before the failure due to disruption of the chemically crosslinked molecular network.

The Young's modulus and the yield stress are proportional to the temperature, as is typically expected for epoxy resin and glassy polymers in general [9]. The peak for the yield stress and the following softening is less prominent in the conditioned samples than in the unconditioned (baseline) samples. This is likely because of the plasticization caused due to the presence of moisture in the conditioned samples. At 95C, the stress-strain curves are different; the conditioned specimen has no clear yield point. Even for the baseline specimen at 95C, the peak for yield stress is not as prominent as at lower temperatures. This vast difference is due to the decrease of glass transition temperature due to moisture. While the baseline specimen is at or near the glass transition temperature of a dry SC-15 resin, the conditioned specimen is significantly over the glass transition temperature. Therefore, no clear yield point is visible.

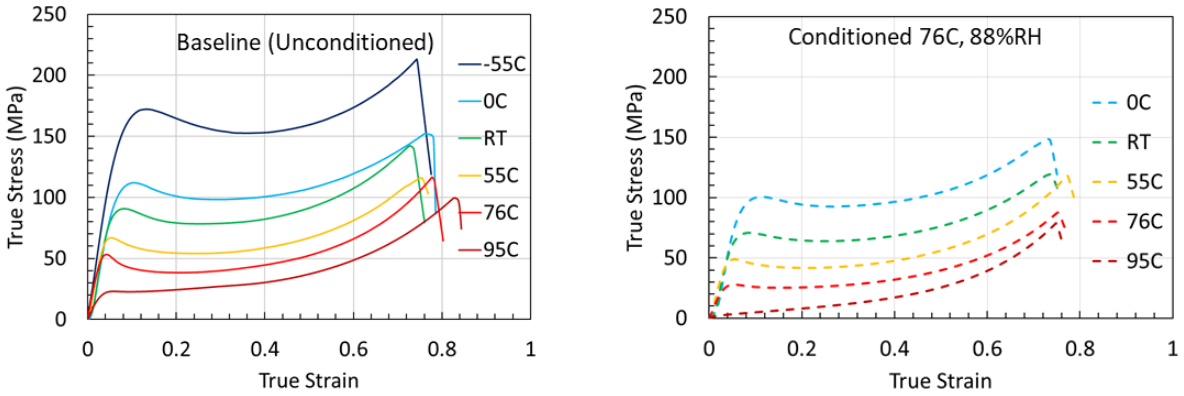

Figure 2. True stress-strain curves at different temperatures for quasistatic compression tests for neat SC-15 resin for (a) baseline (non-conditioned) specimen and (b) specimens conditioned till saturation at 76C, 88%RH (2.1% mass increase).

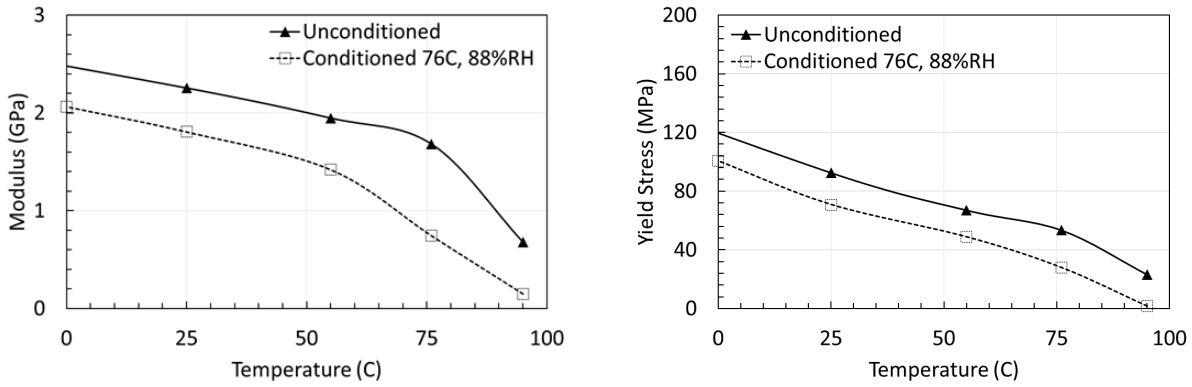

Figure 3. Decrease in (a) modulus and (b) yield stress as a result of an increase in temperature for baseline (unconditioned) and conditioned specimens.

Variations of Young's modulus and yield stress are plotted as a function of temperature in Figures 3(a) and 3(b), respectively. The solid triangles represent the baseline (unconditioned) specimens, and square hollow markers are for the conditioned samples. As expected and evident in the true stress-strain curves, both Young's modulus and yield stress decrease with increasing temperature. For Young's modulus, the reduction is linear till 76C, and then a sharper drop is observed for the test at 95C. This is because the glass transition temperature is ~85-90C.

Interestingly, a similar inflection point or change in slope for the conditioned specimen is observed after the 55C tests. This suggests that the glass transition temperature has been suppressed due to moisture and is now near or below 76C. A similar trend is also observed for yield stress curves but not as prominent. For the conditioned samples tested at 95C, the yield stress tends to zero, similar to the modulus of the conditioned samples at 95C, another indication of the suppression of glass transition temperature and this test being conducted well beyond the glass transition temperature. The stress-strain curve for the 95C specimen looks like a curve for a rubber-like material, with no well-defined yield point and behavior similar to an elastomer subjected to strain hardening.

Figures 4(a) and 4(b) show the true stress-true strain response for tests conducted using the split Hopkinson bar at a strain rate of 3300 s^{-1} for the baseline and conditioned specimens, respectively. As expected, and similar to quasistatic rates, the yield stress is inversely proportional to temperature; it decreases as temperature increases. For the test conducted at cold temperatures, epoxies could be brittle, and the drop in stress post yielding could be due to damage. At room temperature tests, strain softening is observed due to the adiabatic nature of these tests since the test duration is extremely small and the time for heat dissipation is insufficient. Tamrakar et. al. [10] measured the temperature to be 70C for epoxy resin DER 353 when tested at room temperature at a strain rate of 5000 s^{-1}.

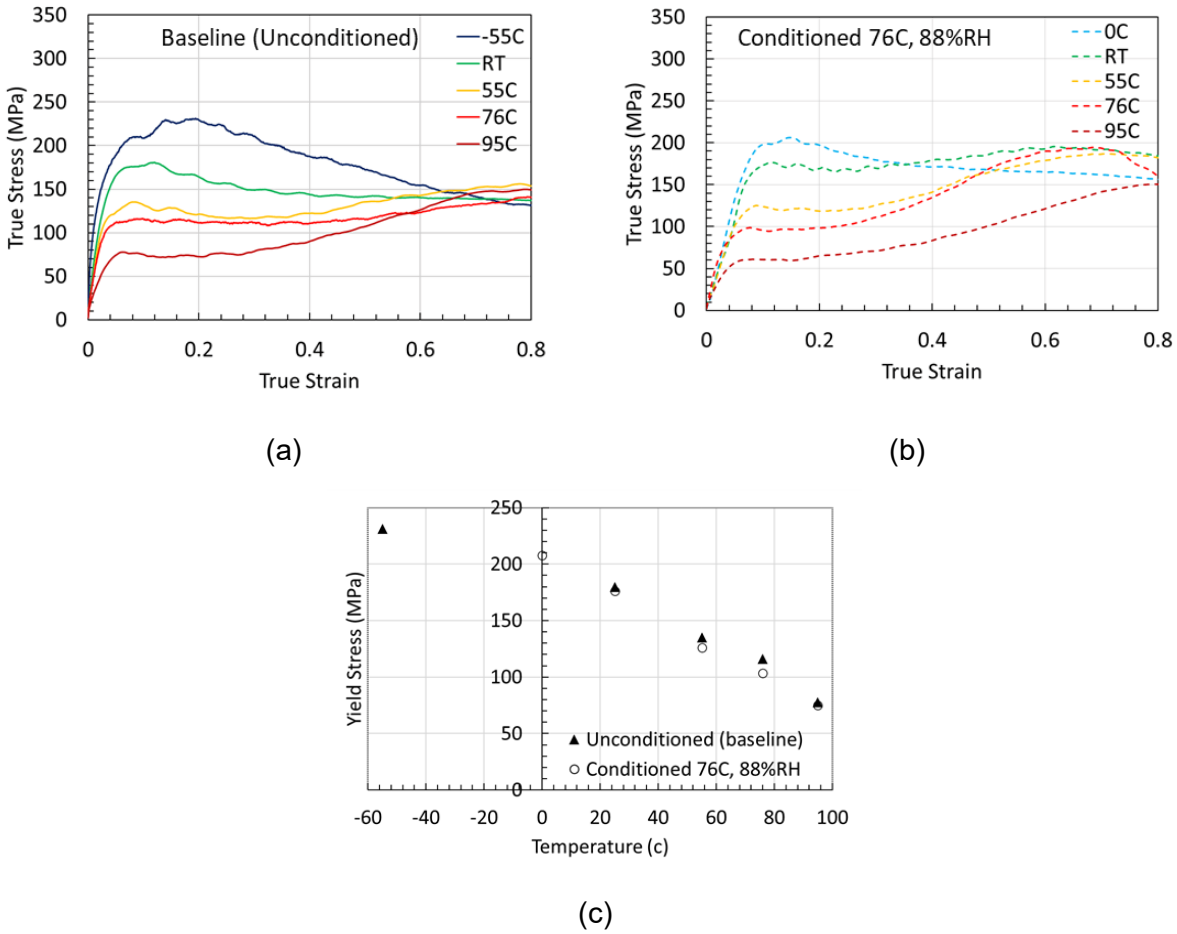

Figure 4. True stress-true strain response of neat SC-15 resin tested using split Hopkinson bar at a strain rate of 3300 s^{-1} at different temperatures for (a) baseline (unconditioned) specimens and (b) conditioned specimens. (c) variation of yield stress with temperature for conditioned and unconditioned specimens.

Figure 4(c) shows the dependence of yield stress on temperature for both baseline (non-conditioned) and conditioned samples. The influence of conditioning and the presence of moisture is not as significant for the tests conducted at high rates. The decrease of yield stress is fairly linear with increasing temperature throughout the range of tests. Interestingly, an inflection in the yield stress vs. temperature curve is not evident for the high rate tests. Additionally, the yield stress values at higher temperatures (95C) do not tend to zero, as observed for the quasistatic tests. This is because the yielding of glass polymers is controlled by more than one energy activation mechanism.

Figure 5 shows the variation of yield stress with average strain rate for three different temperatures, room temperature, -55C, and 76C. The dependence of yield stress on strain rate is easily evident from the figure. The yield stress at room temperature varies from ~75-95 MPa for the quasistatic rates and 160-230 MPa for the high strain rate testing conducted using the Hopkinson bar. The variation of yield stress is bilinear with strain rate due to the two rate processes involved in the deformation. Eyring's initial equation considered only a singular rate process and failed to predict the yield stress accurately; however, the modified Eyring equation – Ree-Eyring [11] can predict the bilinear relationship by assuming two rate processes. These processes are believed to be due to the different types of motion of the molecular chains/segments and not due to the different types of flow units [13].

The modified Eyring equation is given by:

$$\sigma_y(\dot{\varepsilon}T) = \sum_i \frac{2kT}{v_i} \sinh^{-1}\left[\frac{1}{C_i T}\frac{\dot{\varepsilon}}{\dot{\varepsilon}_{0,i}} exp\left[\frac{E_i}{kT}\right]\right]$$

Where the model parameters include activation volume (v_i), activation energy (E_i), pre-exponential factors ($\dot{\varepsilon}_i$) and model constant (Ci). k represents the Boltzmann constant; T is the temperature - 293 K. In our future work, we will use the shifting factors introduced by Bauwens-Crowet et. al. [14] to determine the yield strength as a function of strain rate at a reference temperature (room temperature) and then shift the curves to the operating temperature range (-55C, 76C) and compare it with our experimental results.

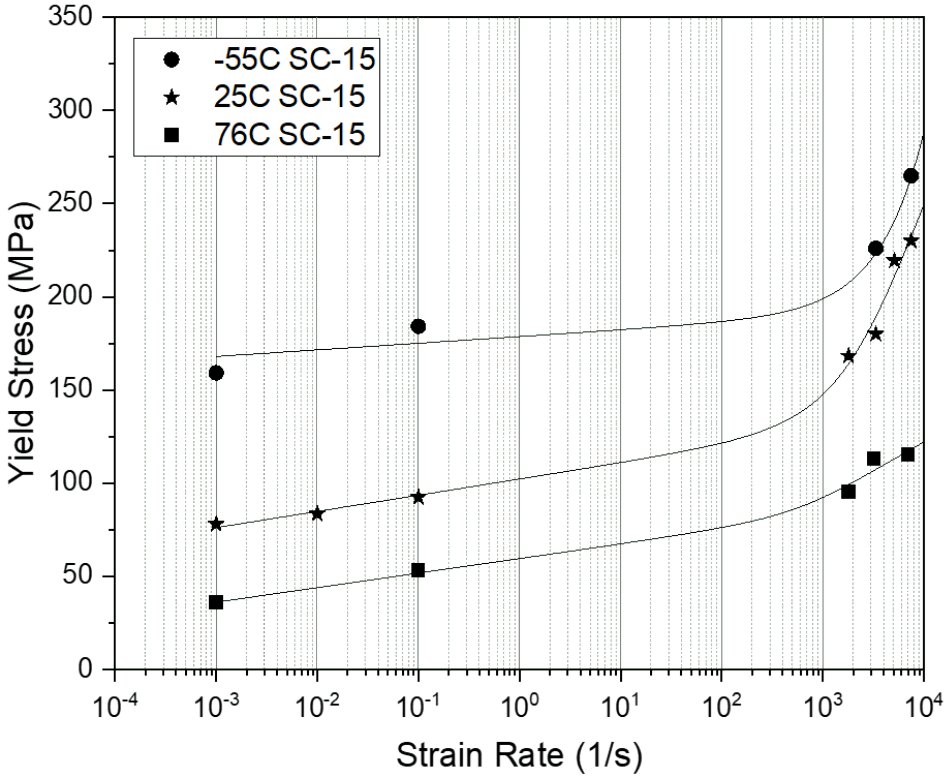

Figure 5. Variation of yield stress with average strain rate using a modified Eyring model for neat SC-15 resin for three different temperatures: -55C, RT, 76C.

Interface Testing using Single Fiber Pullout Tests

Figure 6(a) shows a typical force-displacement curve for a single fiber pullout test. One fiber end is held in the grips and pulled out of the resin. The initial part of the curve is linear, where the fiber-resin interface sees no damage and remains intact. As the load builds up and reaches a threshold value, debonding initiates, i.e., the bond between the fiber and matrix begins to break, and an interfacial crack is initiated. This is an inflection point, and a change in slope is noticeable. From this point onwards, the load is carried through the 'non-damaged' part of the interfacial bond and due to the friction in the debonded part. The load ultimately reaches a peak value, where the crack growth becomes unstable, and the fiber-matrix completely debonds, leading to a sharp drop. The load, however, doesn't drop to zero, and a 'frictional tail force' is noticeable due to the

frictional force between the fiber and the resin. This frictional force gradually decreases to zero as the fiber is completely pulled out of the resin.

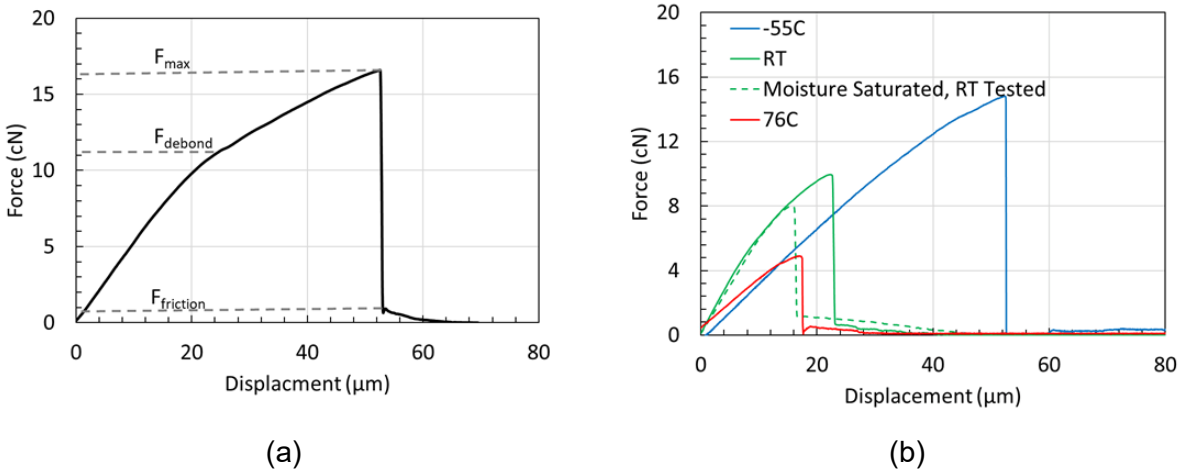

Figure 6. (a) A typical force-displacement curve for single fiber pullout tests and (b) representative force-displacement curves for pullout tests under various environmental conditions.

Figure 6(b) shows the representative curve of each type of pullout test specimen, -55C, RT, 76C, and moisture conditioned tested at RT. Table 2 shows the important test parameters and the apparent IFSS calculated from the force-displacement curves. The embedded length was similar for all test types, ~ 55-60 µm. The fiber diameter is measured for each specimen after failure using an SEM microscope. The IFSS values depend on temperature and moisture, as seen in Figures 6(b) and Table 2. The IFSS values decrease as temperature increases, and the moisture-conditioned specimen sees a decrease of about 26% in IFSS.

Table 2: IFSS, embedded length, and fiber diameter values for the four types of specimens tested at different environmental conditions.*

	-55C	**RT**	**76C**	**2.7% moisture, RT Tested**
IFSS* (MPa)	139.1 ± 22.4	73.24 ± 3.6	40.0 ± 3.8	53.6 ± 2.7
Le (µm)	56.6 ± 10.0	56.6 ± 4.6	61.9 ± 10.5	61.7 ± 20.6
Fiber Dia (µm)	8.98 ± 0.46	8.71 ± 0.56	9.05 ± 0.29	8.81 ± 0.24

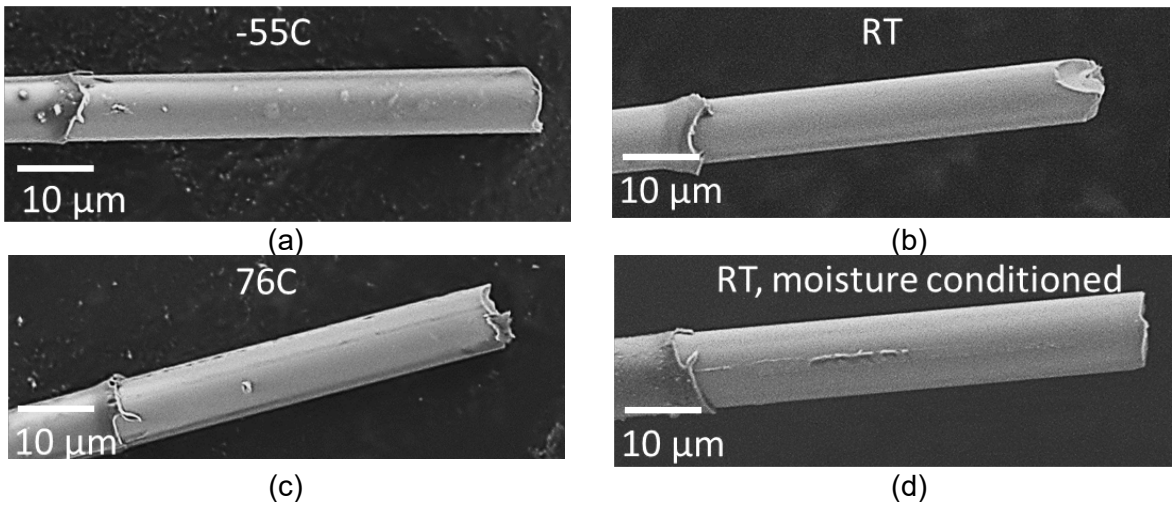

Figure 7. SEM micrographs showing the failure surfaces for all types of test specimens. An interfacial failure is observed for all the test specimens.

Figures 7(a) - (d) show a typical failure surface after a pullout test conducted at -55C, RT, 76C, and moisture conditioned at RT specimens, respectively. A reasonably clean adhesive or an interfacial failure is observed in all cases. However, at higher magnification, there may be evidence of a thin layer of resin on the fiber surface. There are two potential failure modes for debonding governed by the yield stress of the matrix and the peak traction stress describing the onset of progressive failure of the interface (it is common to model interfacial failure using cohesive traction laws where the peak traction is greater than the average IFSS value determined experimentally). Ganesh [13] et. al. considered the ratio of the interface peak traction/resin yield stress (R) to relate material properties to failure mode. In the case of R>1, interfacial failure is preferred. For R<1, debonding will occur in the resin near the fiber surface. The results presented in this paper show that the R-value and the associated failure mode can be expected to be temperature, strain rate, and moisture dependent. It is also noteworthy that during the load drop shown in Figure 6, the strain rate increases significantly due to unstable crack propagation, and one might expect a transition in failure mode along the length of the fiber.

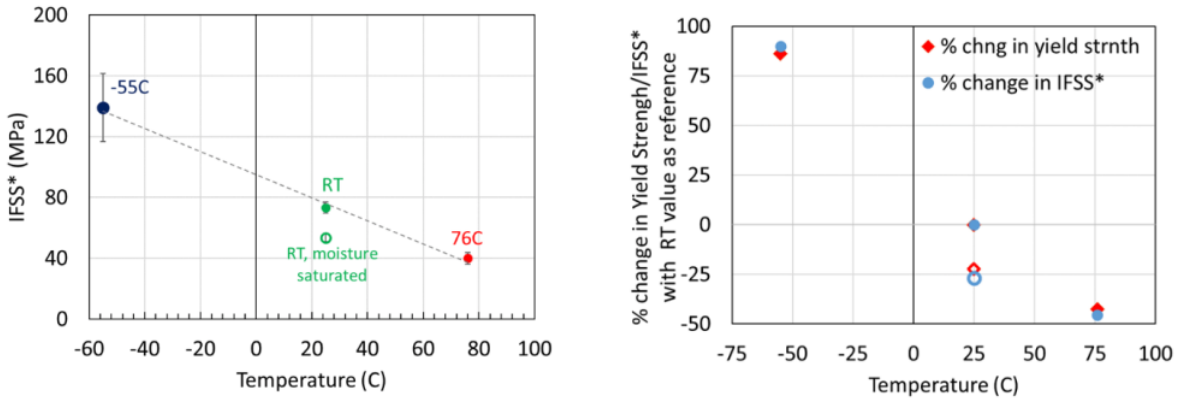

Figure 8. (a) Apparent IFSS plotted against temperature showing a linear correlation and (b) percentage change in apparent IFSS and yield strength calculated using RT value as a reference.

Figure 8(a) shows the plot of apparent IFSS against temperature. IFSS decreases linearly with increasing temperature. The standard deviation for tests conducted at -55C is higher than the other tests for multiple reasons – constituent materials are brittle, and the cold temperatures lead to ice formation on the rubber grips holding the fiber, causing a lot of invalid test failures. Given that the peak loads achieved and therefore the apparent IFSS calculated is affected by yield strength, the percentage change in yield strength and apparent IFSS is plotted in Figure 8(b). The room temperature value is considered the reference (baseline) for both datasets, and percentage change is calculated based on that value. An excellent correlation is observed between the change in IFSS and the change in yield strength. This positive correlation implies that the interfacial failure may be cohesive with a thin resin coating on the fiber since the probability of the temperature dependence of the interphase and the resin being identical is low. This is a topic for more in-depth characterization of the fiber surface.

Low Velocity Impact Tests of Glass Fiber-SC 15 Composites

The force-time and force-displacement curves for the low velocity impact tests conducted on SC-15 composites are shown in figures 9(a) and 9(b). The general trends for specimens at each temperature are similar. As the impactor makes contact, the composite specimen resists it, which increases force. The force reaches the maximum value, and then unloading occurs as the impactor loses contact with the specimen. The maximum force achieved depends on the specimen's stiffness and, therefore, on the temperature at which the test is conducted. The peak force is maximum for the coldest temperature, where specimen stiffness is highest, and the deflection is highest for the 76C specimen with the least stiffness.

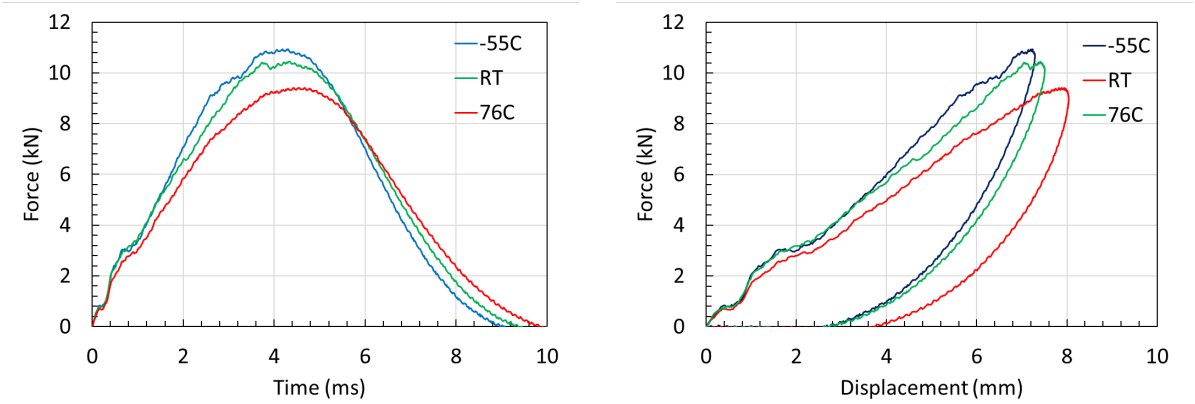

Figure 9. (a) Force-time and (b) force-displacement response of glass fiber-SC-15 composites subjected to 40J impact at room temperature and at the ends of operating temperature range

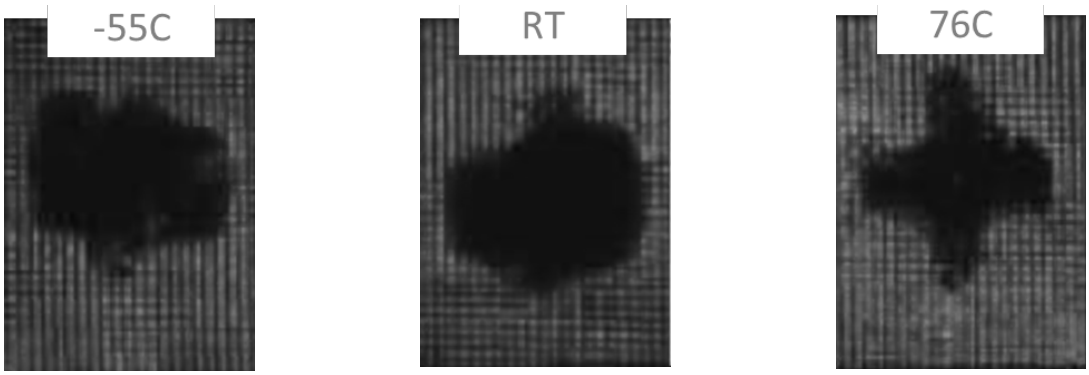

Figure 10. Through thickness C-scans for SC-15 composite specimens subjected to an impact of 40J at (a) -55C, (b) RT, and (c) 76C

Figure 10 shows the ultrasound C-scans through transmission images of the impacted specimens. The dark regions in the pictures show the damage areas or the delaminations caused due to the impact. The damage areas for -55C and RT are comparable and about ~ 20% larger than 76C. A limitation of the through-thickness C-scanning is the inability to detect multiple damage planes. The C-scan will provide the largest delamination area, and other delamination areas smaller than that will remain invisible. Therefore, to compare the damage areas created using these images to characterize the amount of delamination and new surfaces made is inaccurate. The damage areas for -55C and RT show vertical lines near the left and right edge of the specimen. This is because the edges of the specimen were clamped. Once the delamination area has reached the edge, further delamination is prevented due to the clamping. That is also likely why the damage areas for -55C and RT look more circular, whereas, for 76C, it is more prominent along the principal axes. To comment more on the delamination resistance of this composite, additional details such as the area of each delamination should be calculated. Our future work will use the pulse-echo ultrasonic technique to investigate this.

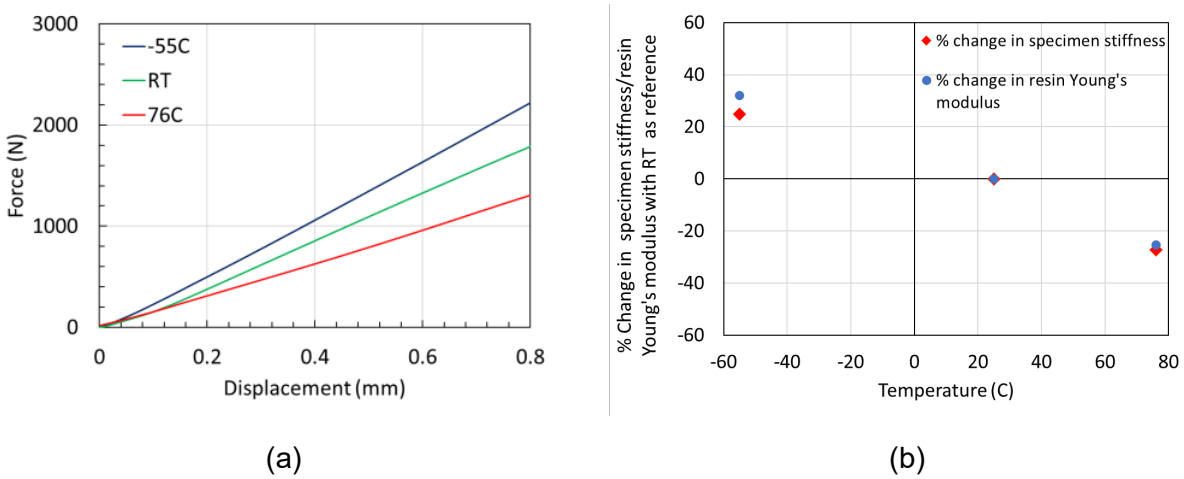

Figure 11. (a) Stiffness of the composite before impact at -55C, RT, and 76C, (b) % change in specimen stiffness, and young's modulus of resin calculated by taking room temperature value as a reference.

Figure 11(a) shows the stiffness of the composite specimens calculated pre-impact. As shown in figure 1(c), the boundary conditions for stiffness testing are the same as that used for LVI tests, clamped on all sides. As intuitively expected and similar to the LVI tests, the stiffness increases as temperature decreases, i.e., the -55C specimen has the highest stiffness. As the loading nose touches the specimen and pushes down on it, the specimen is under transverse loads. These transverse loads cause interlaminar shear deformations and also cause in-plane bending stresses. At higher displacement, it also causes stretching of the layers since the boundaries are clamped. From the above-discussed phenomenon, the resin properties significantly influence the transverse shear deformation of the laminate governed by the interlaminar shear modulus of the composite. Higher resin shear modulus leads to higher composite interlaminar shear stiffness and lesser shear deformation, and an increase in laminate structural stiffness in LVI testing. Figures 11(b) and table 3 show the correlation between specimen stiffness and resin modulus. Considering the room temperature value as a reference, shear modulus increases by 32%, and specimen stiffness increases by 25% at -55C. Similarly, at 76C, both values decrease by 25-27%.

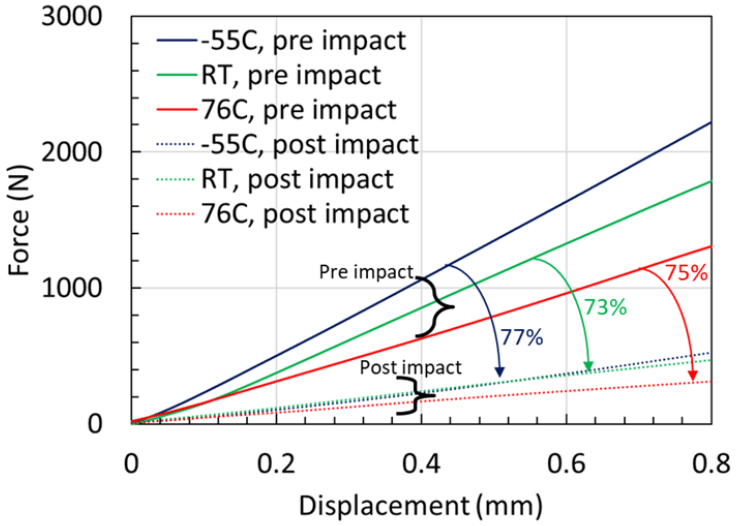

Figure 12. Pre and post impact stiffness for the composites subjected to 40J impacts at the three different temperatures, -55C, RT, and 76C. All specimens suffer about a 75% stiffness degradation due to the impact which is the result of the delaminations of the plies within the composite.

About 75% drop in stiffness is observed for all specimens after impact testing at 40J due to the large delamination areas (Figure 12). The stiffness's absolute value for each specimen depends on the geometry of the panel, clamping conditions, and the amount of energy imparted. For example, the same energy imparted on a thicker specimen would lead to a comparatively lesser stiffness reduction. However, the results represent the damage tolerance of the composites and show that the stiffness change due to impact damage (for 40J) is significantly greater than the stiffness change due to temperature. From an automotive application viewpoint, as more composites are used in the primary structure, often to absorb energy during a crash, the fracture toughness of composites and stiffness retention as a function of temperature and strain rates becomes an important area of research. Typical epoxy resins become brittle as temperature decreases, potentially reducing the fracture toughness and energy absorbing capabilities and affecting safety.

Table 3: Stiffness change due to temperature, impact, change in resin Young's modulus, energy absorbed, and delamination areas for the composite specimens subjected to LVI experiments.

Temperature at which LVI, Stiffness test Conducted	Stiffness (N/mm), Before Impact	% Change in stiffness due to temperature	Youngs Modulus (GPa, (Compression tests of resin)	Shear Modulus, GPa G = E / (2*(1+ν))	Stiffness (N/mm), After Impact, Tested at -55, RT and 76C	% Stiffness Loss Due Damage from Impact	Energy Absorbed (J)	Delamination Area (c-scan) mm²
-55C	2753	+24.8	2.97 (+32.0 %)	1.09	638	76.8	26.2	4261
RT	2205	0	2.25	0.82	591	73.2	26.5	4453
76C	1605	-27.2	1.68 (-25.3%)	0.61	393	75.4	29.6	3441

Summary and Next Steps

The effect of environmental factors on the mechanical properties of the composites and their constituent materials, resin, and the interface is investigated. Neat resin, fiber-resin interface, and composites are tested at room temperature and the ends of the operating temperature range. The resin properties are characterized using uniaxial compression tests at various strain rates and saturated moisture. Key properties such as yield stress and modulus are calculated at different temperatures, and the influence of moisture on glass transition temperature and mechanical properties are also shown. Interface properties are characterized using single fiber pullout tests to calculate the apparent IFSS. IFSS shows a linear dependence on temperature for this specific resin-fiber combination and shows a good correlation with yield stress. Composites are subjected to low velocity impact tests at room temperature and the ends of the operating temperature range. The stiffness change due to temperature and impact damage is evaluated. The change in stiffness due to temperature correlates well with resin Young's modulus.

Since all the constituent materials play an integral role in both structural integrity and energy absorbing capabilities, characterization of the influence of environmental factors provides critical insights into the durability, damage tolerance, and performance of these composites in a wide range of atmospheres. To design a component that can enhance and maintain the functional integrity in a temperature range of -55C to 76C, a resin with a higher glass transition temperature than SC-15 would serve better. Since the pullout tests showed an adhesive failure at all temperatures, the interface of the glass fabric has the potential to be tailored by depositing silanes to improve the interfacial bonding and enhance energy absorbing capabilities. To improve damage tolerance and impact resistance at frigid temperatures, resins with higher fracture toughness should be developed, or alternative means could be used, such as placing a compliant interlayer to enhance decoupling and reduce transverse shear stresses.

Acknowledgements

The research was sponsored by the U.S. Army CCDC Army Research Laboratory and was accomplished under Cooperative Agreement Number W911NF-18-2-0299.

The views and conclusions contained in this document are those of the authors and should not be interpreted as representing the official policies, either expressed or implied, of the Army Research Laboratory or the U.S. Government. The U.S. Government is authorized to reproduce and distribute reprints for Government purposes, notwithstanding any copyright notation herein.

The authors would also like to thank undergraduate interns Lorrha Hitchner, Dean Vanegas, and Megan Monteleone for their help with specimen fabrication and testing.

Bibliography

1. "Department of Defense Test Method Standard - Environmental Engineering Considerations and Laboratory Tests" MIL-STD-210G 2008.
2. Smerd, R., et al. "High strain rate tensile testing of automotive aluminum alloy sheet." International Journal of Impact Engineering 32.1-4 (2005): 541-560.
3. Ganesh, Raja, Subramani Sockalingam, and John W. Gillespie. "Dynamic effects of a single fiber break in unidirectional glass fiber-reinforced polymer composites: Effects of matrix plasticity." Journal of Composite Materials 52.14 (2018): 1873-1886.
4. Tamrakar, Sandeep, et al. "Rate dependent mode II traction separation law for S-2 glass/epoxy interface using a microdroplet test method." Composites Part A: Applied Science and Manufacturing 124 (2019): 105487.
5. Doshi S.M, Sharma S., Morris K., Deitzel J. M., Yarlagadda S and Gillespie Jr J.W., "Peel Strength of Glass Fiber-Epoxy Composites with Thermoplastic Interlayers under Different Environmental Conditions", SAMPE Conference Proceedings. Charlotte, NA, May 23-26, 2022.
6. Doshi, S. M., Manoharan, N., Haque, B. Z. G., Deitzel, J. M., & Gillespie Jr, J. W. (2021). Investigating the Influence of Environmental Conditioning on Epoxy Resins at Quasistatic and High Strain Rates for Material Operating Limit. In Proceedings of the American Society for Composites—Thirty-Sixth Technical Conference on Composite Materials.
7. Chen, Branndon R., et al. "Interfacial Shear Strength (IFSS) and Absorbed Energy Versus Temperature in Carbon Fiber-Thermoplastic Composites via Single Fiber Pullout Testing." Proceedings of the American Society for Composites—Thirty-fifth Technical Conference. 2020.
8. Doshi, Sagar M., et al. " Low velocity impact experiments of S-2 glass-epoxy composites under different environmental conditions." Proceedings of the American Society for Composites—Thirty-Seventh Technical Conference on Composite Materials. 2022.
9. R. S. Hoy and M. O. Robbins, "Strain hardening in polymer glasses: Limitations of network models," Phys. Rev. Lett., vol. 99, no. 11, p. 117801.
10. S. Tamrakar, R. Ganesh, S. Sockalingam, B. Z. Haque, and J. W. Gillespie, "Experimental Investigation of Strain Rate and Temperature Dependent Response of an Epoxy Resin Undergoing Large Deformation," J. Dyn. Behav. Mater., vol. 4, pp. 114–128, 1234, doi: 10.1007/s40870-018-0144-8.
11. Ree, Taikyue, and Henry Eyring. "Theory of non-newtonian flow. i. solid plastic system." Journal of Applied Physics 26.7 (1955): 793-800.
12. Roetling, J. A. "Yield stress behaviour of poly (ethyl methacrylate) in the glass transition region." Polymer 6.11 (1965): 615-619.
13. Bauwens-Crowet, C., Jean Claude Bauwens, and Georges Homes. "Tensile yield-stress behavior of glassy polymers." Journal of Polymer Science Part A-2: Polymer Physics 7.4 (1969): 735-742.